Infrared Spectra of RuTPP, RuCOTPP, and $Ru(CO)_2TPP$ Isolated in Solid Argon

Lahouari Krim,*,† Sébastien Sorgues,‡ Benoit Soep,§ and Niloufar Shafizadeh‡

L.A.D.I.R./U.M.R. 7075 CNRS-Université Pierre et Marie Curie, Boîte 49, 4 Place Jussieu, 75252 Paris, Cedex 05, France, Laboratoire de Photophysique Moléculaire. U.P.R. 3361 CNRS, Bat 210 Université de Paris-Sud, 91405 Orsay, Cedex, France, and Laboratoire Francis Perrin Bat 522 DRECAM/SPAM CEA Saclay, 91191 Gif sur Yvette, France

Received: March 15, 2005

Infrared spectra of unstable species such as CO-free ruthenium tetraphenylporphyrin RuTPP and RuCOTPP (species with vacant coordination sites) isolated in solid argon at 8 K have been recorded. Selective deposition conditions allow the isolation of either RuTPP and RuCOTPP or RuCOTPP and $Ru(CO)_2TPP$. This depends on the preparation conditions of the sample. A specific Ru−CO bending mode has been characterized at 590.1 cm^{-1} for $Ru(CO)_2TPP$. The behavior of each vibrational mode of RuTPP, RuCOTPP, and $Ru(CO)_2TPP$ has been analyzed. Modes such as γ_8 at 721.3 cm^{-1} (out-of-plane stretching mode $\gamma_{(C\beta-H)sym}$) and ν_{41} at 1342.8 cm^{-1} ($\nu_{C\alpha-N}$ coupled with $\delta_{C\alpha-Cm}$) reflect the charge transfer in the porphyrin. Indeed, the addition of one or two CO ligands to RuTPP reduces the charge transfer between the metal center and the porphyrin, which appears as an increase in the frequency of the ν_{41} mode and in a decrease in that of the γ_8 mode.

Introduction

Ru-metalloporphyrins are interesting analogues of heme metalloporphyrins in that they can easily fix a ligand on the Ru^{II} atom. Further analogy comes with the easy fixation at the II-oxidation state, as for the site Fe^{II} in heme. There is still a need to study the structure and reactivity of these porphyrins to determine the ligand exchange properties. Matrix isolation and IR spectroscopy are an ideal tool for this purpose as metal−ligand bands can be isolated and followed in time as a reaction proceeds.

Reactions with RuTPP[1−10] have been subject to several studies. Proniewicz et al.[2] reported infrared and resonance Raman spectra of films of dioxygen adducts and oxo complexes of RuTPP at 45 K, and Mu et al.[3] combined FTIR, UV−vis, and ESR spectroelectrochemistry with microvoltammetry and classical electrochemical techniques to elucidate the electron-transfer mechanism for the oxidation and reduction of RuCOTPP in different nonaqueous solvents. Brown et al.[5] studied the effect of extraplanar ligands on the site of oxidation in Ruthenium porphyrins. Salzmann et al.[8] synthesized and characterized via single-crystal X-ray diffraction methods RuCOTPP(1-methylimidazole)/chloroform.

The X-ray study of Cullen et al.[9] has led to the geometry of dicarbonyl $Ru(CO)_2TPP$, containing markedly bent Ru−C−O bonds (154°). Eaton et al.[1,10] showed that in carbonylporphyrin prepared in CO atmosphere a strong peak assigned to the dicarbonyl species and a very weak peak assigned to the monocarbonyl species were observed. Maintaining the sample under a dry nitrogen atmosphere resulted in a rapid loss of the dicarbonyl peak, while the return of the sample to a CO atmosphere resulted in the growth of the dicarbonyl peak and the diminution of the monocarbonyl peak.

During the purification steps, the ruthenium carbonyl porphyrin usually picks up bases such as water or ethanol. The preparation of dicarbonyl complexes followed by removal of the second carbonyl group in vacuo provides a route to complexes with a sixth vacant coordination site.

With the matrix isolation technique, we can study unstable species such as RuTPP and RuCOTPP and observe the transformation between a mono and dicarbonylporphyrin. In this study, we report the IR spectra of RuTPP, RuCOTPP, and $Ru(CO)_2TPP$ species.

Experimental Section

Argon gas, was provided by "L'Air liquide" with a purity of 99.9995%. RuCOTPP was purchased from SIGMA-Aldrich and was purified by sublimation prior to use. Spectra were recorded using an FTIR Bruker spectrometer (IFS 113HR) at 0.5 cm^{-1} resolution in the 400−4000 cm^{-1} range. For each sample, corresponding to different concentrations of RuTPP, RuCOTPP, and $Ru(CO)_2TPP$, two kinds of spectra were recorded at 8 K, after each of the following procedures: (1) Directly after sample deposition and (2) after warming up the matrix in several steps up to 35 K to vary and monitor the formation of higher stoichiometry complexes.

Preparation of the Sample. The X-ray study of Cullen et al.[9] has shown that the ruthenium carbonyl−porphyrin complexes are mainly made up as L-Ru−COTPP and $Ru(CO)_2TPP$, where L is bases such water or ethanol. The complex was thus heated from a Knudsen cell at 450−550 K under vacuum at 10^{-7} mbar for 3−6 h to remove adsorbed bases (passivation). The resulting complex was vaporized then at 600 K and was co-deposited with pure argon onto a cryogenic metal mirror maintained around 8 K (the pressure during matrix deposition did not exceed 10^{-5} mbar). Deposition times were around 30 min. The vaporization conditions are varied to favor $Ru(CO)_2TPP$ and RuCOTPP or CO-free RuTPP and RuCOTPP. Two different vaporization conditions have been used.

Conditions A: Isolation of $Ru(CO)_2TPP$ and RuCOTPP. Passivation in vacuo of the ruthenium carbonyl−porphyrin

* To whom correspondence should be addressed. E-mail: krim@ccr.jussieu.fr.
† Université Pierre et Marie Curie.
‡ Université de Paris-Sud.
§ Laboratoire Francis Perrin.

10.1021/jp0580930 CCC: $30.25
Published on Web 08/27/2005

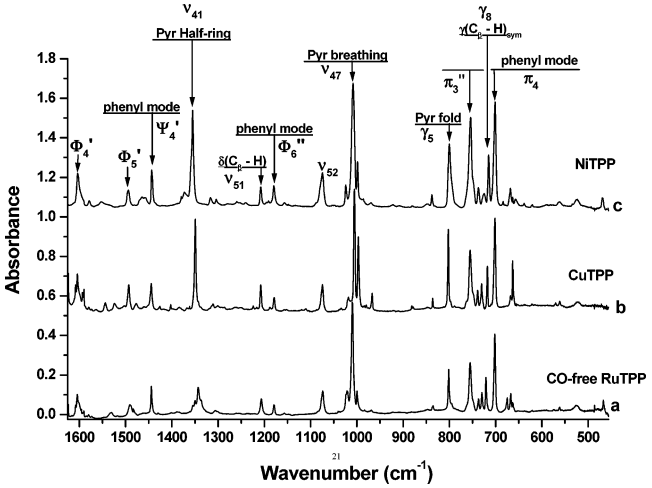

Figure 1. IR spectra of metal-TPP in argon matrix at 8 K: (a) CO-free RuTPP, (b) CuTPP, (c) NiTPP.

complexes at 450 K allows to remove the bases without loosing the CO molecules. The IR spectra recorded during the passivation show no signal in the CO stretching region at 1900−2200 cm^{-1}. After 3 h of heating at 450 K, all the bases are removed from the ruthenium carbonyl−porphyrin complex. The purity of the sample was confirmed spectroscopically (impurities and removed bases bands were observed in 1700−1600 cm^{-1} and 900−1200 cm^{-1} regions). The evaporation and deposition under these conditions (labeled conditions A) at 600 K shows that the isolated species in the argon matrix are the free CO molecules, RuCOTPP, and Ru(CO)$_2$TPP complexes.

The high concentration of CO molecules in the matrix allows a total recombination (RuTPP + CO) and the formation of RuCOTPP and Ru(CO)$_2$TPP ([Ru(CO)$_2$TPP]/[RuCOTPP] ∼ 2). No free RuTPP is detected under these experimental conditions.

Conditions B: Isolation of CO-Free RuTPP and RuCOTPP. Long heating times at higher temperatures, approximately 6 h at 550 K, under vacuum allows the removal of a maximum number of CO molecules (IR spectra recorded during the passivation show an increasing signal of free CO stretching band at 2137.2 cm^{-1}). The loss of the axial CO molecules, under these experimental conditions (labeled conditions B), enables the isolation of the CO-free RuTPP and RuCOTPP in the argon matrix at 8 K. Indeed, during the evaporation of the porphyrin at 600 K, we detect mainly CO-free RuTPP and traces of RuCOTPP because of the recombination of the residual free CO in the matrix. Very small quantities of Ru(CO)$_2$TPP are detected under these experimental conditions ([Ru(CO)$_2$TPP]/[RuCOTPP] ∼ 0.01).

Results

(a) RuTPP. Figure 1, taken under conditions B, shows the IR spectrum of what we shall assign to RuTPP in the argon matrix, in the range 400−1700 cm^{-1}. This spectrum (Figure 1a) is compared with the spectra of different porphyrins such as CuTPP (Figure 1b) and NiTPP (Figure 1c). The three spectra resemble each other, and this is a result of the weak influence of the metal center on the vibrational modes of the skeleton of the molecule. Relying on a DFT study of NiTPP,[11] we could make a good analysis of the three porphyrins. Table 1 gathers various vibrational mode assignments of these species. In the following, we will take the 700−800 cm^{-1} spectral region as a characteristic domain of the specific vibrational modes of the porphyrin skeleton.

(b) RuCOTPP and Ru(CO)$_2$TPP. These complexes are characterized by the CO stretching modes in the region between 1900 and 2140 cm^{-1}. Measurements made in solution[5] and in solid[1,10] phases gave for RuCOTPP species a frequency of 1930 and 1945 cm^{-1}, respectively, for the CO stretching mode. The

TABLE 1: Vibrational Modes (Frequencies Are in cm^{-1}) of NiTPP, CuTPP, and RuTPP Isolated in Argon Martix

mode and symmetry	local coordinate	NiTPP[a]	NiTPP	CuTPP	RuTPP
Ψ_1[c]	out-of-plane phenyl mode	(3063)	3065.4	3066.8	3069.4
Φ_4' (B_{2g}), Φ_4'' (E_u)	in-plane phenyl mode	1599	**1603.3**[d]	**1601.4**	**1604.6**
Ψ_3'' (E_g)	out-of-plane phenyl mode	1576	1578.5	1578.2	1579.9
ν_{38} (E_u)[b]	$\nu(C_\alpha\text{-}C_\beta)$	1550	1552.1	1542.9	1532.3
Φ_5'' (E_u)	out-of-plane phenyl mode	1491	**1493.9**	**1491.9**	**1491.8**
ν_{39} (E_u)	$\nu(C_\alpha\text{-}C_m)_{sym}$	1456	1464.4	1477.1	1462.7
Ψ_4' (A_{2u}), Ψ_4'' (E_g)	out-of-plane phenyl mode	1440	**1443.3**	**1443.7**	**1445.1**
ν_{29} (B_{2g})	ν(Pyr quarter-ring)	1377	1379.5	1402.9	1390.4
ν_{41} (E_u)	$\nu(\text{Pyr half-ring})_{sym}$	1351	**1354.9**	**1349.1**	**1342.8**
ν_{40} (E_u)	ν(Pyr quarter-ring)	1317	1317.0	1310.1	1308.4
ν_{51} (E_u)	$\delta(C_\beta\text{-}H)_{asym}$	1207	**1207.7**	**1208.1**	**1207.0**
ν_{34} (B_{2g})	$\delta(C_\beta\text{-}H)_{asym}$	1190	1191.6	1186.7	
Φ_6'' (E_u)	in-plane phenyl mode	1177	**1179.4**	**1178.4**	**1178.8**
Ψ_7'' (E_g)	out-of-plane phenyl mode	1158	1156.7	1156.1	1157.6
ν_{52} (E_u)	$\delta(C_\beta\text{-}H)_{sym}$	1077	**1074.9**	**1074.5**	**1073.9**
ν_{44} (E_u), ν_{30} (B_{2g})	$\nu(\text{Pyr half-ring})_{asym}$	1023	1023.9	1017.8	1021.4
ν_{47} (E_u)	ν(Pyr breathing)	1007	**1008.3**	**1005.9**	**1009.9**
Φ_8'' (E_u)	in-plane phenyl mode	998	998.5	996.7	999.6
ν_{46} (E_u)	$\delta(\text{Pyr def})_{asym}$	840	838.2	835.8	835.9
γ_5 (A_{2u})	Pyr fold_{sym}	794	**800.0**	**802.3**	**801.5**
π_3'' (E_u)	in-plane phenyl mode	745	**754.1**	**754.9**	**755.6**
π_3 (B_{1g})	in-plane phenyl mode	742	737.3	738.8	737.1
γ_{20} (E_g)	Pyr fold_{asym}	725	725.0	730.1	729.5
γ_8 (A_{2u})	$\gamma(C_\beta\text{−}H)_{sym}$	708	715.1	718.2	721.3
π_4 (B_{1g}), π_4'' (E_u)	in-plane phenyl mode	696	**701.1**	**702.1**	**701.6**
Φ_9'' (E_u)	in-plane phenyl mode	666	668.0	663.2	667.3
π_5' (A_{2g})	in-plane phenyl mode	(565)	563.0	561.2	561.7
π_5'' (E_u)	in-plane phenyl mode	525	525.2	522.5	525.2
ν_{49} (E_u)	δ(Pyr rot)	466	469.5		467.2

[a] Mode frequencies measured in the solid phase by Rush et al.[11] [b] ν_i and γ_i skeletal porphyrin modes. ν_i: Modes, in-plane skeletal porphyrin, such as $\nu_{C\alpha-Cm}$, δ(pyrol def). γ_i: Modes, out-of-plane skeletal porphyrin, such as (pyrol fol), γ_{Ni-N}. [c] Φ, Ψ, π, and σ phenyl modes. Φ and Ψ: Modes in the phenyl plane. π and σ: Modes out of the phenyl plane. [d] The strongest features in the infrared spectra are in bold.

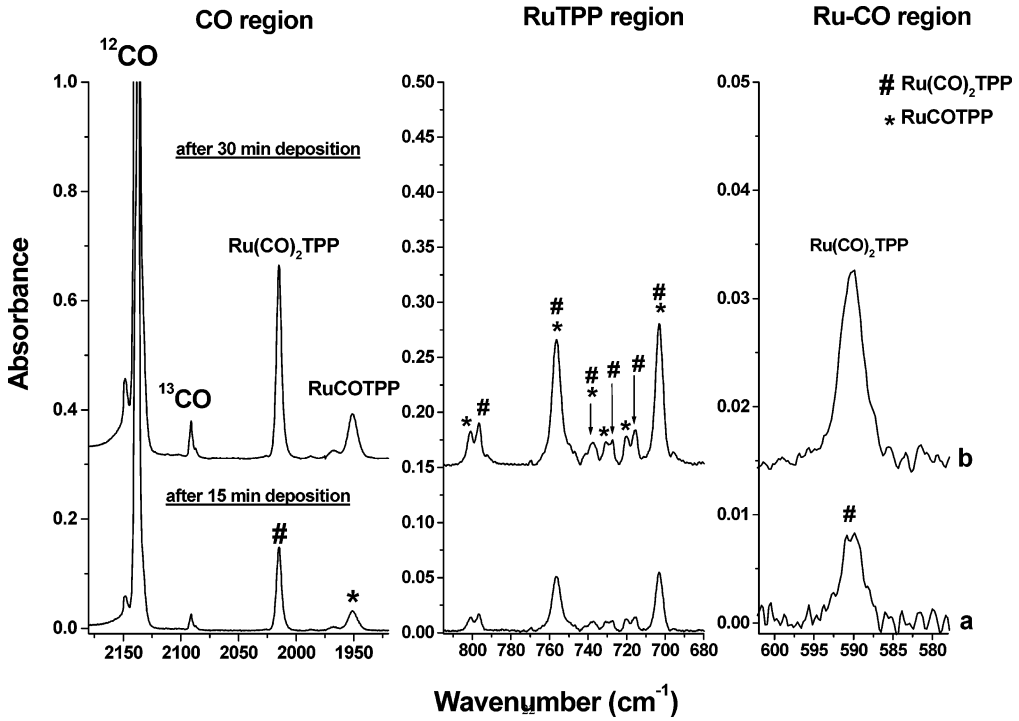

Figure 2. IR spectra of the ligated porphyrin in argon matrix at 8 K: (a) after 15 min deposition and (b) after 30 min deposition. All detected bands grow up with the same behavior. #, $Ru(CO)_2TPP$; *, RuCOTPP.

following assignment will be made here, on the basis of deposition time effects and temperature effects upon the nature of the deposited species.

Figure 2 taken under conditions A shows the evolution of the spectrum as a function of the deposition time of the ligated porphyrin. All detected bands grow up with the same behavior. In the CO stretching region (Figure 2a and Figure 2b), a great quantity of free ^{12}CO molecules is observed at 2137.2 cm^{-1}, and traces of free ^{13}CO are observed at 2090.7 cm^{-1}. CO stretching frequency modes for RuCOTPP and $Ru(CO)_2TPP$ are observed at 1951.1 and 2015.1 cm^{-1}, respectively. These frequencies are similar to those reported by Eaton et al.[1,10] in solid phase (RuCOTPP at 1945 cm^{-1} and $Ru(CO)_2TPP$ at 2005 cm^{-1}).

In the region of porphyrin vibrational modes (700−800 cm^{-1}), the spectrum is similar with that of the free RuTPP. However, most of the bands are doublets which indicates that porphyrin skeletal modes are sensitive to the number of CO adducts. A new band attributed to a ligated porphyrin is detected at 590.1 cm^{-1} (Figure 2a and 2b). This band does not exist in the IR spectrum of the free RuTPP.

On the other hand, Figure 3, taken under conditions B, shows the evolution of the spectrum as a function of deposition time of the CO-free porphyrin. Indeed, during the deposition of the CO-free RuTPP, all detected bands do not show the same behavior. In the CO stretching region (1900−2140 cm^{-1}), the bands remain almost constant, even after 60 min deposition, whereas in the region of the porphyrin modes (700−800 cm^{-1}), the bands grow enormously (only the free RuTPP is evaporated, most of the CO has been dissociated from the porphyrin). We cannot thus distinguish any signal at 590 cm^{-1} in these conditions.

The preceding assignments have been made on the basis of the following arguments:

In Figure 2, bands due to RuCOTPP and $Ru(CO)_2TPP$ grow up similarly in every spectral region, while in Figure 3 only bands in the free RuTPP spectral region (700−800 cm^{-1}) increase strongly and could be easily attributed to RuTPP species.

Comparing Figures 2a and 3a, bands with the same intensity after 15 min deposition should belong to RuCOTPP (these bands are different from those already attributed to CO-free RuTPP species), while the others present only in Figure 2a are due to $Ru(CO)_2TPP$ species. This rests upon the fact that in the CO stretching region at 1951.1 cm^{-1}, the intensity is the same for the RuCOTPP complex (in Figures 2a and 3a).

Finally, the intensity of the new band observed at 590.1 cm^{-1} correlates with the $Ru(CO)_2TPP$ bands. This is due probably to the antisymmetric bending mode (Ru−CO) in $Ru(CO)_2TPP$. Spiro et al.[12] have measured a frequency at 578.0 cm^{-1} for the bending mode of Ru−CO in the ruthenium−octaethylporphyrin $Ru(CO)_2OEP$ in solution by resonance Raman. Nakamoto et al.[13,14] observed the antisymmetric bending mode (Fe−CO) of $Fe(CO)_2TPP$ at 583.0 cm^{-1}.

Matrix Temperature Effects. Evaporation of ligated porphyrins at 600 K under conditions A allows the isolation of RuCOTPP and $Ru(CO)_2TPP$ in argon matrixes. Because of the high concentration of free CO in the matrix, no CO-free RuTPP species are observed. Under these conditions, Figure 4 shows the effect of warming the matrix from 8 to 30 K. It is seen that the bands due to $Ru(CO)_2TPP$ become stronger while the bands due to RuCOTPP decrease. At high temperatures (30 K), the matrix is not rigid and the free monomeric CO diffuses and reacts with the five-coordinate RuCOTPP to form the six-coordinate $Ru(CO)_2TPP$. These phenomena have been observed by Nakamoto et al.[13] in the case of FeCOTPP, who focused their studies on the assignment of TPP-ligand vibrations rather than on the vibrations originating from TPP itself.

The high concentration of CO in the matrix allows us to treat [CO] as a constant, and the concentrations of RuCOTPP and $Ru(CO)_2TPP$ are given by their integrated intensities of the CO stretching bands at 1951.1 and 2015.1 cm^{-1}, respectively. Figure

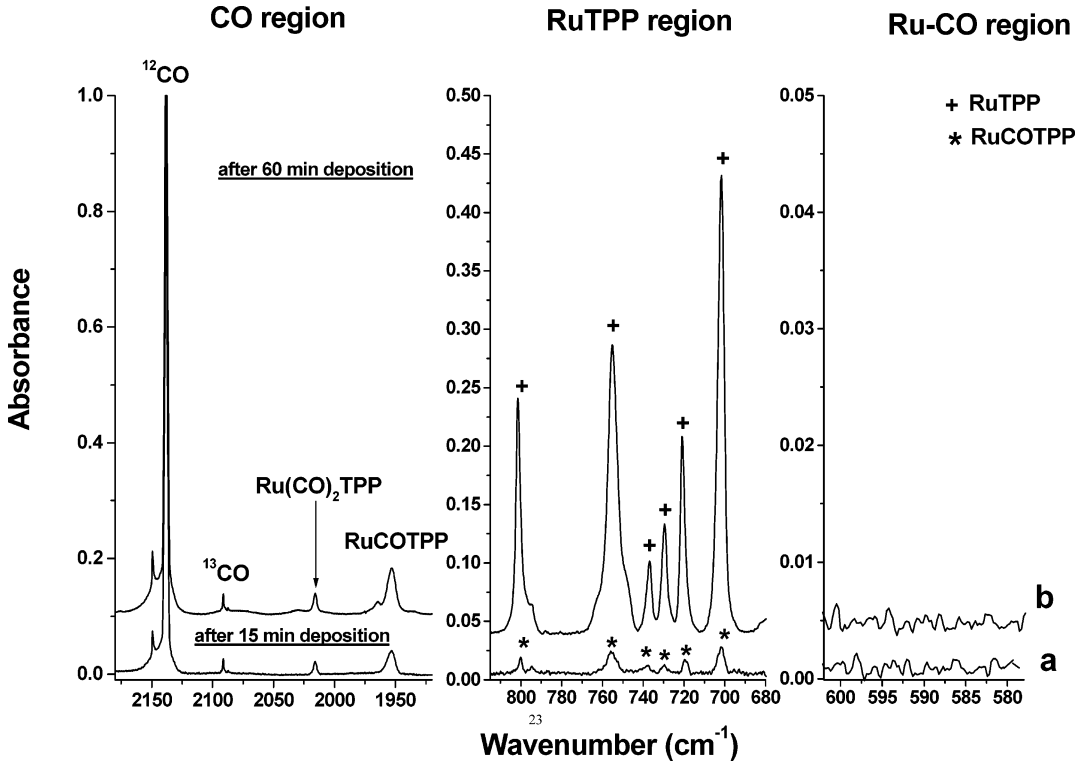

Figure 3. IR spectra of CO-free porphyrin RuTPP in argon matrix at 8 K: (a) after 15 min deposition and (b) after 60 min time deposition. Only the bands due to the CO-free porphyrin RuTPP grow up strongly. *, RuCOTPP; +, CO-free RuTPP.

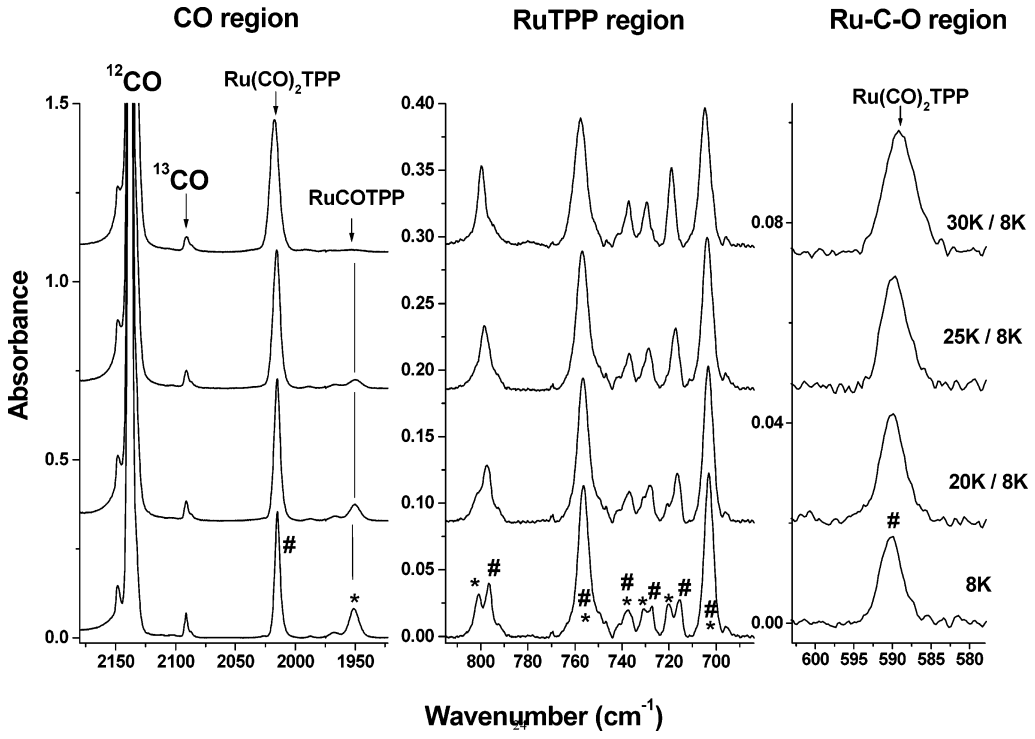

Figure 4. Effect of warming the matrix from 8 K to 30 K. All bands due to RuCOTPP disappear at 30 K. #, $Ru(CO)_2TPP$; *, RuCOTPP.

5 shows the effect of warming the matrix from 8 to 35 K on the relative intensities of the CO stretching bands.

These observations allow the assignment of the RuCOTPP and $Ru(CO)_2TPP$ bands to be confirmed. All decreasing bands are due to RuCOTPP species, while increasing bands are due to $Ru(CO)_2TPP$ species. Combining the observations of the bands from Figures 2−4, we were able to separate the three species $Ru(CO)_2TPP$, RuCOTPP, and RuTPP and make a reliable spectral assignment of each species. Figure 6 gathers some spectral regions of RuCOTPP, $Ru(CO)_2TPP$, and RuTPP. Table 2 lists all vibrational mode frequencies of the three species.

Discussion

Characterization of the RuCOTPP and $Ru(CO)_2TPP$. We have shown in the Results section that conditions can be found to isolate either $Ru(CO)_2TPP$ and RuCOTPP (conditions A) or free CO RuTPP and RuCOTPP (conditions B).

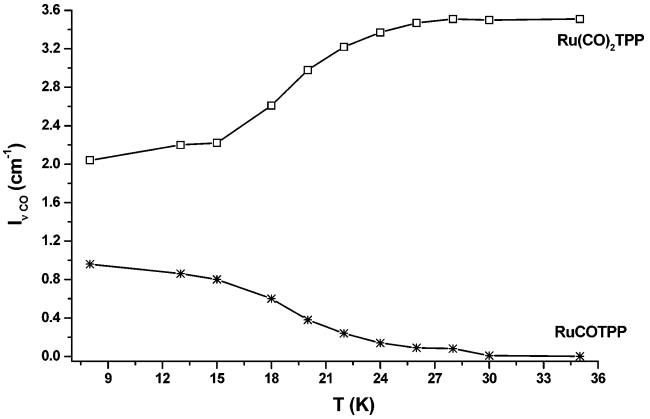

Figure 5. Measured intensities of ν_{CO} modes of $Ru(CO)_2TPP$ and RuCOTPP at different temperatures of argon matrix. Open squares indicate the $Ru(CO)_2TPP$. Stars indicate the RuCOTPP.

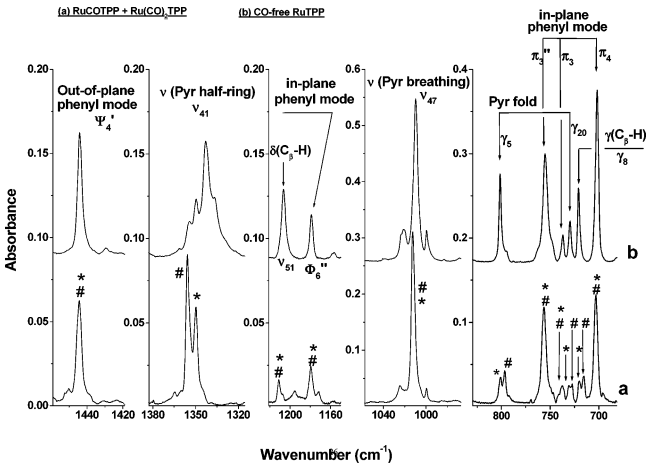

Figure 6. IR spectra in argon matrix at 8 K of (a) $Ru(CO)_2TPP$ + RuCOTPP and (b) CO-free porphyrin RuTPP. #, $Ru(CO)_2TPP$; *, RuCOTPP.

(1) Spectral Shifts on ν_{CO}. Previously, Wayland et al.[15] observed in the solid state the ν(CO) of $Fe(CO)_2TPP$ and FeCOTPP at 2042 and 1973 cm^{-1}, respectively. They also found the equilibrium constant for the formation of the monoadduct and the biscarbonyl adduct to be 6.6 10^4 and 140, respectively. Nakamato et al.[13,14] observed in the argon matrix the ν(CO) of $Fe(CO)_2TPP$ and FeCOTPP at 2064 and 2000 cm^{-1}, respectively. The ν(CO) in the argon matrix is blue shifted by 22 and 27 cm^{-1} for $Fe(CO)_2TPP$ and FeCOTPP, respectively, from that in the solid state. Eaton et al.[1,10] measured ν(CO) for $Ru(CO)_2TPP$ and RuCOTPP in the solid state at 2005 and 1945 cm^{-1}, respectively, while we observed ν(CO) at 2015.1 and 1951.1 cm^{-1} for $Ru(CO)_2TPP$ and RuCOTPP, respectively, in argon matrix. One can notice that from the solid sate to the argon matrix ν(CO) is 10 cm^{-1} blue shifted for $Ru(CO)_2TPP$ and only 6 cm^{-1} for RuCOTPP.

In general, ν(CO) is governed by two factors[16]: (1) σ donation from CO to the metal which tends to increase ν(CO) and is maximized at the M−C−O angle of 120° and (2) π-back-donation from the metal to CO which tends to decrease ν(CO) and is maximized at the M−C−O angle of 180°. ν(CO) in the 1:2 adduct is always higher than in the 1:1 adduct. This is understandable since the second CO group decreases the degree of π-back-bonding because of competition between two trans CO groups.

(2) Skeletal Modes of the $Ru(CO)_xTPP$ Porphyrin. DFT calculations show that the D_{4h} symmetry of NiTPP[11] (constructed with a planar porphyrin ring and its phenyl rings set perpendicular to the prophyrin) is not the lowest energy structure. They predict that NiTPP will lower its energy by 0.61 kcal/mol by adopting a D_{2d} type geometry and 1.69 kcal/mol by adopting the S_4 one. IR spectra in the solid phase and infrared intensity calculations done by Rush et al.[11] confirm that multiple conformations of NiTPP may be present in solution, and in view of the small energy differences predicted by DFT, S_4, D_{2d}, and D_{4h} geometries should be appreciably populated. According to the vibrational assignments of Rush et al.,[11] modes are labeled as follows:

(i) The in-plane skeletal porphyrin modes, such as $\nu_{C\alpha-Cm}$, δ(pyrol def), are labeled ν_1, while the out-of-plane skeletal porphyrin modes, such as (pyrol fol), $\gamma_{metal-N}$, are labeled γ_i.

(ii) The phenyl modes are labeled Φ, Ψ, π, and σ. The Φ and Ψ modes are in the phenyl plane, while the π and σ are phenyl out-of-plane modes.

Table 1 lists the mode frequencies measured in the solid phase for NiTPP (by Rush et al.[11]) and our results in the argon matrix. Our experimental results are quite similar to those observed by Rush et al.;[11] there are two new experimental frequencies predicted by Rush et al.[11] at 3063 cm^{-1} (out-of-plane phenyl mode) and 565 cm^{-1} (in-plane phenyl mode) and measured by us at 3065.4 and 563.0 cm^{-1}, respectively.

Relying on the predictions of the NiTPP DFT calculations, we can compare the vibrational frequencies of RuTPP, CuTPP, and NiTPP on one hand and on the other hand we can also analyze the behavior of each vibrational mode of RuTPP, RuCOTPP, and $Ru(CO)_2TPP$ species.

Infrared spectra of NiTPP, CuTPP, and RuTPP in argon matrixes are similar. One can also compare the vibrational frequencies between each species. For each species, the strongest features in the infrared spectra are the skeletal modes ν_{41} (sym Pyr half-ring), ν_{51} (asym $\delta_{C\beta-H}$), ν_{52} (sym $\delta_{C\beta-H}$), ν_{47} (Pyr breathing), and γ_5 (sym Pyr fold) and the phenyl mode pairs ϕ_4', ϕ_5'', Ψ_4', π_3, π_4 (Figure 1). They do not seem to depend strongly on the nature of the metal except the mode ν_{41} (sym Pyr half-ring), measured at 1354.9 cm^{-1} in the NiTPP spectrum that shifts to 1349.1 cm^{-1} for CuTPP and to 1342.8 cm^{-1} for RuTPP. The vibration assigned as ν(sym Pyr half-ring) corresponds to $\nu(C_\alpha-N)$ coupled with $\delta(C_\alpha-C_m)$ (C_m, meso carbon);[17,18] its downshifted frequency reflects the charge transfer from the metal to the porphyrin. Decreasing charge transfer from the metal to the porphyrin causes shortening of the $C_\alpha-N$ bond, leading to an increase of the ν_{41} frequency.[17−18] Comparing ν_{41} frequencies for each species shows that the charge transfer is higher in RuTPP and lower in NiTPP porphyrin.

Table 2 lists all observed vibrational frequencies of RuTPP, RuCOTPP, and $Ru(CO)_2TPP$ species. The bands located at $\Psi_3'' = 1579.9$ cm^{-1}, $\Phi_8'' = 999.6$ cm^{-1}, and $\pi_5'' = 525.2$ cm^{-1}, attributed to the phenyl modes, are not sensitive to adducted CO while most of the vibrational bands of the free porphyrin exibit blue or red shift when CO interacts with RuTPP. However, only the band located at 1342.8 cm^{-1} and those observed in the 700−800 cm^{-1} spectral area are sensitive to the number of adducting CO.

(3) Strong Charge-Transfer Effects on Vibrational Mode Frequencies. When adducting CO to RuTPP, the band attributed to ν_{41} ($\nu_{C\alpha-N}$ coupled with $\delta_{C\alpha-Cm}$) at 1342.8 cm^{-1} shows the greatest shift for the skeletal vibrational modes of the free porphyrin. The band is 7.3 cm^{-1} blue shifted from RuTPP to RuCOTPP and 13.1 cm^{-1} blue shifted from RuTPP to $Ru(CO)_2TPP$. The ν_{41} frequency increase in the $Ru(CO)_{1-2}TPP$ species indicates that the interaction of Ru with one or two CO

TABLE 2: Vibrational Modes (Frequencies Are in cm^{-1}) of RuTPP, RuCOTPP, and $Ru(CO)_2TPP$ Isolated in Argon Martix

mode and symmetry	local coordinate	RuTPP	RuCOTPP	$Ru(CO)_2TPP$
CO stretching	C−O		**1951.1**[c]	**2015.1**
Φ_4' (B_{2g}), Φ_4'' (E_u)[b]	in-plane phenyl mode	**1604.6**	**1601.1**	**1601.1**
			(−3.5)[d]	(−3.5)
Ψ_3'' (E_g)	out-of-plane phenyl mode	1579.9	1579.9	1579.9
			(0)	(0)
ν_{38} (E_u)[a]	$\nu(C_\alpha-C_\beta)$	1532.3	1532.9	1532.9
			(+0.6)	(+0.6)
Φ_5'' (E_u)	out-of-plane phenyl mode	**1491.8**	**1492.7**	**1492.7**
			(+0.9)	(+0.9)
ν_{39} (E_u)	$\nu(C_\alpha-C_m)_{sym}$	1462.7	1462.9	1462.9
			(+0.2)	(+0.2)
Ψ_4' (A_{2u}), Ψ_4'' (E_g)	out-of-plane phenyl mode	**1445.1**	**1444.3**	**1444.3**
			(−0.8)	(−0.8)
ν_{41} (E_u)	ν(Pyr half-ring)$_{sym}$	1342.8	1350.1	1355.9
			(+7.3)	(+13.1)
ν_{40} (E_u)	ν(Pyr quarter-ring)	1308.4	1308.9	1308.9
			(+0.5)	(+0.5)
ν_{51} (E_u)	δ $(C_\beta-H)_{asym}$	**1207.0**	**1211.4**	**1211.4**
			(+4.4)	(+4.4)
Φ_6'' (E_u)	in-plane phenyl mode	**1178.8**	**1179.7**	**1179.7**
			(+0.9)	(+0.9)
ν_{52} (E_u)	δ $(C_\beta-H)_{sym}$	**1073.9**	**1075.6**	**1075.6**
			(+1.7)	(+1.7)
ν_{44} (E_u), ν_{30} (B_{2g})	ν(Pyr half-ring)$_{asym}$	1021.4	1024.7	1024.7
			(+3.3)	(+3.3)
ν_{47} (E_u)	ν(Pyr breathing)	**1009.9**	**1012.8**	**1012.8**
			(+2.9)	(+2.9)
Φ_8'' (E_u)	in-plane phenyl mode	999.6	999.6	999.6
			(0)	(0)
ν_{46} (E_u)	δ(Pyr def)$_{asym}$	835.9	837.2	835.7
			(+1.3)	(−0.2)
γ_5 (A_{2u})	Pyr fold$_{sym}$	**801.5**	**801.0**	**796.6**
			(-0.5)	(−4.9)
π_3'' (E_u)	in-plane phenyl mode	**755.6**	**756.5**	**756.5**
			(+0.9)	(+0.9)
π_3 (B_{1g})	in-plane phenyl mode	737.1	736.3	736.3
			(−0.8)	(−0.8)
γ_{20} (E_g)	Pyr fold$_{asym}$	729.5	730.8	727.4
			(+1.3)	(−2.1)
γ_8 (A_{2u})	$\gamma(C_\beta-H)_{sym}$	721.3	720.2	715.5
			(−1.1)	(−5.8)
π_4 (B_{1g}), π_4'' (E_u)	in-plane phenyl mode	701.6	703.3	703.3
			(+1.7)	(+1.7)
Φ_9'' (E_u)	in-plane phenyl mode	667.3	666.3	666.3
			(−1)	(−1)
antisymmetric bending	Ru−C−O			590.1
π_5'' (E_u)	in-plane phenyl mode	525.2	525.2	525.2
			(0)	(0)
ν_{49} (E_u)	δ(Pyr rot)	467.2	467.2	467.2
			(0)	(0)

[a] ν_i and γ_i: skeletal porphyrin modes. ν_i: Modes, in-plane skeletal porphyrin, such as $\nu_{C\alpha-Cm}$, δ(pyrol def). γ_i: Modes, out-of-plane skeletal porphyrin, such as (pyrol fol), γ_{Ni-N}. [b] Φ, Ψ, π, and σ: phenyl modes. Φ and Ψ: Modes in the phenyl plane. π and σ: Modes out of the phenyl plane. [c] Strongest features in the infrared spectra are in bold. [d] Spectral shifts between RuTPP and $Ru(CO)_{1-2}TPP$ are in parentheses.

(CO is a strong π-acceptor ligand) reduces the charge transfer from Ru to the porphyrin (see Figure 6 and Table 2). Indeed, the frequency of the ν_{41} mode decreases when the charge transfer is important. One measures a frequency of 1342.8 cm^{-1} for RuTPP, 1349.8 cm^{-1} for CuTPP, and 1354.9 cm^{-1} for NiTPP, which indicates a higher charge transfer in the RuTPP adducts. The addition of one or two CO to RuTPP results in an increase in the frequency of the ν_{41} mode from 1350.1 cm^{-1} (RuCOTPP) to 1355.9 cm^{-1} ($Ru(CO)_2TPP$). The increase in the ν_{41} mode is due to the competition for electrons between the CO ligands and the macrocycle. The presence of ligands deprives the cycle, and less charge is injected in the antibonding orbitals thus increasing their frequency.

Conversely, the frequency of the out-of-plane stretching mode $\gamma(C_\beta-H)$sym increases when the amount of charge transfer increases. The behavior of this mode is exactly opposite to that of the ν_{41} mode. One measures a frequency of 721.3 cm^{-1} for RuTPP, 718.2 cm^{-1} for CuTPP, and only 715.1 cm^{-1} for NiTPP where charge transfer is weakest. As the addition of one or two CO reduces the charge transfer, the out-of-plane stretching mode $\gamma(C_\beta-H)$sym, located at $\gamma_8 = 721.3$ cm^{-1}, is 1.1 and 5.8 cm^{-1} red shifted for RuCOTPP and $Ru(CO)_2TPP$, respectively (Figure 6).

(4) Weaker Charge-Transfer Effects on Vibrational Mode Frequencies. The bands attributed to skeletal vibrational modes of RuTPP, located at $\nu_{38} = 1532.3$ cm^{-1} (mode $\nu_{C\alpha-C\beta}$), $\nu_{39} = 1462.7$ cm^{-1} (symmetric mode $\nu_{C\alpha-Cm}$), $\nu_{40} = 1308.4$ cm^{-1} (mode $\nu_{C\alpha-C\beta}$ coupled with ν_{Cm-H}), $\nu_{51} = 1207.0$ cm^{-1} (asymmetric mode $\delta_{C\beta-H}$), $\nu_{52} = 1073.9$ cm^{-1} (symmetric mode $\delta_{C\beta-H}$), $\nu_{44} = 1021.4$ cm^{-1} (mode $\nu_{C\beta-H}$ coupled with $\nu_{C\alpha-N}$), and $\nu_{47} = 1009.9$ cm^{-1} (pyrol breathing) are blue shifted when one or two CO are added. The measured shifts range between

0.5 and 4.4 cm^{-1}. The bands attributed to the phenyl modes of RuTPP and located at $\Phi_5'' = 1491.8\ cm^{-1}$, $\Phi_6'' = 1178.8\ cm^{-1}$, $\pi_3'' = 755.6\ cm^{-1}$, and $\pi_4 = 701.6\ cm^{-1}$ are blue shifted, while those located at $\Phi_4' = 1604.6\ cm^{-1}$, $\psi_4' = 1445.1\ cm^{-1}$, $\pi_3 = 737.1\ cm^{-1}$, and $\Phi_9'' = 667.3\ cm^{-1}$ are red shifted. Measured shifts range between 0.8 and 3.5 cm^{-1}. These bands are not sensitive to the number of adducting CO. In the low-frequency region, 840−720 cm^{-1}, the observed bands depend on the number of ligating CO: The band attributed to the asymmetric pyrolle deformation and located at $\nu_{46} = 835.9\ cm^{-1}$ is 1.3 cm^{-1} blue shifted for RuCOTPP and 0.2 cm^{-1} red shifted for Ru-$(CO)_2$TPP; the band attributed to the asymmetric pyrolle folding located at $\gamma_{20} = 729.5\ cm^{-1}$ is 1.3 cm^{-1} blue shifted for RuCOTPP and 2.1 cm^{-1} red shifted for $Ru(CO)_2$TPP; and the band attributed to the symmetric pyrolle folding and located at $\gamma_5 = 801.5\ cm^{-1}$ is red shifted by 0.5 and 4.9 cm^{-1} for RuCOTPP and $Ru(CO)_2$TPP, respectively.

While comparing the mode frequencies of CuTPP, NiTPP, RuTPP, and $Ru(CO)_{1-2}$TPP, all these modes quoted in this part do not translate concretely the charge-transfer effect between the metal center and the porphyrin. This is opposite to the γ_8 and ν_{41} modes whose displacements reflect clearly this phenomenon.

Conclusion

Upon the preparation conditions of the sample, unstable species (with vacant coordination sites) such as CO-free RuTPP and RuCOTPP have been isolated in argon matrix. The specific vibrational frequency of the metal ligand has been observed and assigned to the bending mode in $Ru(CO)_2$TPP complex. Vibrational analysis of the skeletal modes of the free CO RuTPP and those of ligated porphyrins $Ru(CO)_{1-2}$TPP have revealed the classical metal−ligand electron transfer, causing considerable shifts in frequencies of the γ_8 (out-of-plane stretching (C_β-H)-sym) and ν_{41} (sym Pyr half-ring) modes located at 721.3 and 1342.8 cm^{-1}, respectively. Decreasing charge transfer from the metal to the porphyrin causes an increase of the frequency of ν_{41} mode and a decrease of that of γ_8 mode. The observation of the variations of these mode frequencies can inform directly about the state of the charge transfer in systems such as metalloporphyrins or ligated metalloporphyrins.

References and Notes

(1) Bonnet, J. J.; Eaton, S. S.; Eaton, G. R.; Holm, R. H.; Ibers, J. A. *J. Am. Chem. Soc.* **1973**, *95*, 2141.
(2) Proniewicz, L. M.; Paeng, I. R.; Lewandowski, W.; Nakamoto, K. *J. Mol. Struct.* **1990**, *219*, 335.
(3) Mu, X. H.; Kadish, K. *Langmuir* **1990**, *6*, 51.
(4) Deng, Y. J.; Mu, X. H.; Tagliatesta, P.; Kadish, K. M. *Inorg. Chem.* **1991**, *30*, 1957.
(5) Brown, G. M.; Hopf, F. R.; Ferguson, J. A.; Meyer, T. J.; Whitten, D. G. *J. Am. Chem. Soc.* **1973**, *95*, 5939.
(6) Cheng, R.; Lin, S.; Mo, H. *Organometallics* **1997**, *16*, 2121.
(7) Lorkovic, I.; Ford, P. *Inorg. Chem.* **1999**, *38*, 1467.
(8) Salzmann, R.; Ziegler, Ch. J.; Godbout, N.; Mcmahon, M. T.; Suslick, K. S.; Oldfield, E. *J. Am. Chem. Soc.* **1998**, *120*, 11323.
(9) Cullen, D.; Meyer, E.; Srivastara, T. S, Jr.; Tsutsui, M. *J. Chem. Soc., Chem. Commun.* **1972**, 584.
(10) Eaton, G.; Eaton, S. *J. Am. Chem. Soc.* **1975**, *97*, 235.
(11) Rush, T. S.; Kozolowski, P. M.; Piffat, C. A.; Kumble, R.; Zgierski, M. Z.; Spiro, T. *J. Phys. Chem. B* **2000**, *104*, 5020.
(12) Kim, D.; Su, Y. O.; Spiro, T. G. *Inorg. Chem.* **1986**, *25*, 3993.
(13) Kuroi, T.; Oshio, H.; Nakamoto, K. *J. Phys. Chem.* **1985**, *89*, 4087.
(14) Proniewicz, L.; Kuroi, T.; Nakamoto, K. *J. Mol. Struct.* **1990**, *238*, 1.
(15) Wayland, B. B.; Mehne, L. F.; Swartz, J. *J. Am. Chem. Soc.* **1978**, *100*, 2379.
(16) Kozuka, M.; Nakamoto, K. *J. Am. Chem. Soc.* **1981**, *103*, 2162.
(17) Abe, M.; Kitagawa, T.; Kyogoku, Y. *J. Chem. Phys.* **1978**, *69*, 4526.
(18) Kitagawa, T.; Abe, M.; Ogoshi, H. *J. Chem. Phys.* **1978**, *69*, 4516.